Contact planarization of ensemble nanowires

2011 Nanotechnology 22 245304

(http://iopscience.iop.org/0957-4484/22/24/245304)

Nanotechnology **22** (2011) 245304 (6pp) doi:10.1088/0957-4484/22/24/245304

Contact planarization of ensemble nanowires

A C E Chia and R R LaPierre

Department of Engineering Physics, Centre for Emerging Device Technologies, McMaster University, Hamilton, ON, L8S 4L7, Canada

E-mail: lapierr@mcmaster.ca

Received 18 February 2011, in final form 29 March 2011
Published 21 April 2011
Online at stacks.iop.org/Nano/22/245304

Abstract

The viability of four organic polymers (S1808, SC200, SU8 and Cyclotene) as filling materials to achieve planarization of ensemble nanowire arrays is reported. Analysis of the porosity, surface roughness and thermal stability of each filling material was performed. Sonication was used as an effective method to remove the tops of the nanowires (NWs) to achieve complete planarization. Ensemble nanowire devices were fully fabricated and I–V measurements confirmed that Cyclotene effectively planarizes the NWs while still serving the role as an insulating layer between the top and bottom contacts. These processes and analysis can be easily implemented into future characterization and fabrication of ensemble NWs for optoelectronic device applications.

(Some figures in this article are in colour only in the electronic version)

1. Introduction

Since the discovery of the vapor–liquid–solid (VLS) mechanism [1], semiconductor nanowires (NWs) have been studied as a novel candidate for many potential applications such as transistors [2], sensors [3], lasers [4] and perhaps most interestingly, solar cells [5, 6]. Semiconductor NW devices can be broadly categorized into single or ensemble NW devices. While the fabrication of most single NW devices employs traditional semiconductor processing methods (such as contact formation by electron beam lithography), the fabrication of ensemble NW devices presents a new set of technical challenges [7]. In particular, the performance of ensemble NW devices may be limited by the high sheet resistance of front contacts due to poor interconnection of contact material among the NWs [8] and shunting paths present between the front electrode on top of the NWs and the rear electrode consisting of the substrate on which NWs are grown [9]. These challenges can be addressed by the addition of an inactive, support medium to fill the space between the NWs [10]. The presence of this filling medium isolates the front and back contacts of the device to prevent shunting [11], while also planarizing the NW array to allow the deposition of a planar front contact with low sheet resistance on top of the NWs [12].

Planarization of ensemble NWs using both inorganic and organic filling materials has been reported previously [12–19]. Among inorganic filling materials, silicon dioxide (SiO_2) and spin on glass (SOG) have been most extensively studied [12, 13]. Chemical vapor deposition (CVD) of SiO_2 resulted in a conformal deposition which made filling difficult for tall NWs and created voids in the SiO_2 which in turn caused delamination during subsequent processing [14]. For SOG, planarization was difficult to achieve for a dense array of thin NWs [14]. Among organic filling materials, some success has been achieved by using poly(methyl methacrylate) (PMMA) [15, 16], polydimethylsiloxane (PDMS) [17], accuflow T-27 (Honeywell) [14] and Cyclotene resin (DOW chemical) [18] as filling materials. Conversely, other inorganic materials have faced many challenges. Spin coated polystyrene caused bundling of NWs due to capillary forces [19], while spin coated Shipley 1518 photoresist left voids between tall wires [10]. Despite these varying degrees of success, there has been no consistent study comparing the suitability of different inorganic materials as a feasible filling medium for planarization. Additionally, there has been no established standard by which the effectiveness of planarization can be assessed.

In this paper, we examine the viability of four different transparent, organic polymers as candidate filling materials for radial GaAs–AlInP heterostructured NWs. The studied organic polymers include S1808 photoresist from Shipley, SC200 from Silecs, SU8-2 from Microchem and Cyclotene 3022-35

Table 1. Outline of spin coating parameters for each filling material.

		S1808	SC200	SU8	Cyclotene
Spin	Duration (s)	30	20	60	60
	Speed (rpm)	4000	2000	3000	3000
Softbake	Duration (min)	2	5	4	1.5
	Temperature (°C)	110	150	95	100
Hardbake	Duration (min)	2	5	5	30
	Temperature (°C)	130	200	200	250

from DOW Chemical. Unlike previous studies, we will both qualitatively analyze the thermal stability and porosity of each polymer while quantitatively examining the surface roughness to assess the suitability of a material as a filling medium for planarization. Finally, a novel approach of sonication after the addition of the filling medium will be explored as the penultimate processing step towards fabrication of ensemble NW devices.

2. Experimental details

The radial GaAs–AlInP heterostructured NWs were grown by VLS in a gas source molecular beam epitaxy (MBE) system. Before growth, an n-doped (111)B GaAs substrate with an approximate doping density of 1×10^{18} cm^{-3} was cleaned by a 20 min UV ozone, a subsequent 30 s buffered HF bath and a final 10 min rinse in deionized (DI) water. Then, 1 nm of Au was evaporated onto the substrate to serve the role of seed particles for VLS NW growth. The substrate was then placed into the MBE system where it was prepared for growth by degassing and plasma cleaning as described elsewhere [5], followed by the NW growth. The NW structure consisted of an n-doped GaAs core covered by a nominally undoped AlInP shell. The n-doped GaAs core was grown at 575 °C for 25 min with a two-dimensional (2D) equivalent growth rate of 1 μm h^{-1} and a V/III flux ratio of 2.3. The GaAs core was Te-doped at a nominal doping density of 1×10^{18} cm^{-3} as determined by previous thin film calibrations. The undoped, lattice-matched AlInP shell was grown at 500 °C for 20 min with a 2D film growth rate of 0.5 μm h^{-1} and a V/III flux ratio of 3.45. This structure was grown for future optoelectronic device studies with AlInP as a window layer. However, the procedures described here are equally applicable to other NW structures. The as-grown NWs shown schematically in figure 1(a) were then characterized using a JEOL JSM-7000F scanning electron microscope (SEM).

After growth and characterization by SEM, a series of processing steps was performed on the NW ensemble to achieve a planar contact that interconnects the NW array at the top. First, ~0.5 ml of each of the four polymers (S1808, SC200, SU8 and Cyclotene) was dispensed across individual ensemble NW samples using a syringe such that each polymer uniformly covered each sample. Each polymer was then allowed to sit for 5 min to seep to the bottom of the NWs in an effort to minimize voids in the subsequent film. To achieve the structure shown schematically in figure 1(b), each NW sample was then spin coated with different spinning and curing parameters (outlined in table 1) as recommended by the manufacturer. It must be noted that prior to spin coating the Cyclotene, a layer of adhesion promoter (AP3000 from DOW Chemical) was spun on the NWs at 2000 rpm for 20 s. Additionally, the Cyclotene hard bake was done in a nitrogen glovebox environment with an oxygen concentration of less than 100 ppm at a slow temperature ramp of 5 °C min^{-1} as recommended by the manufacturer. Following the spin coat,

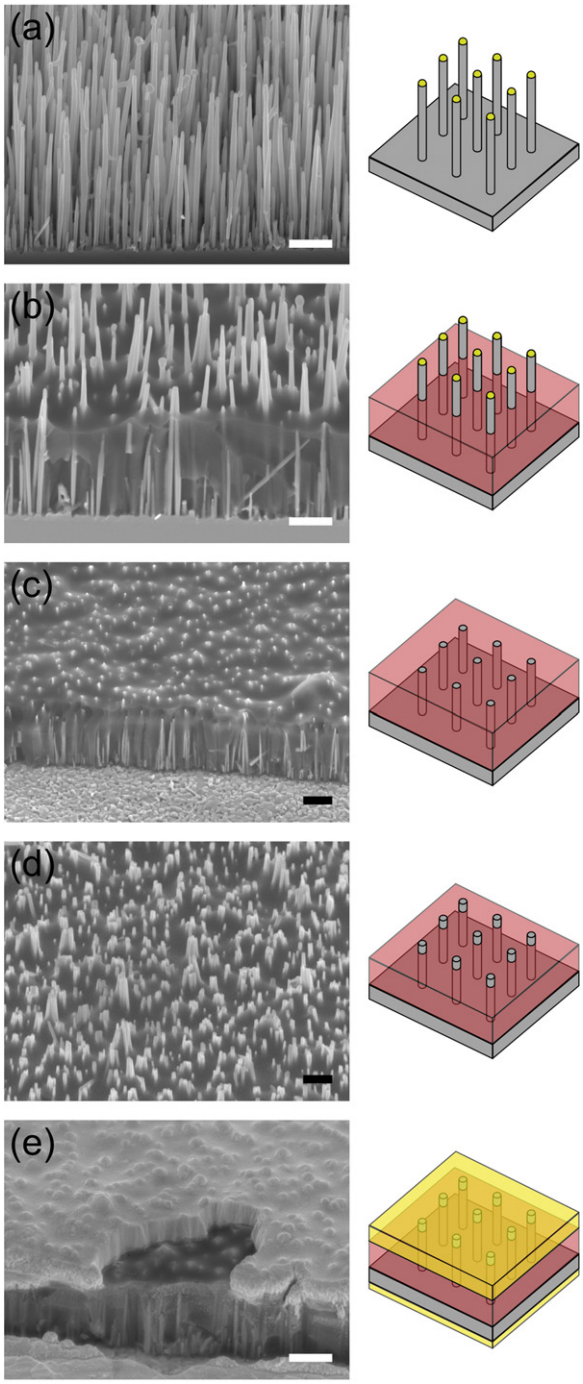

Figure 1. 45° tilted SEM images and schematics of the NW ensemble (a) directly after growth, (b) after spin coating with Cyclotene, (c) after sonication in DI water, (d) after reactive ion etching (RIE) and (e) after contact deposition and annealing. The actual contacts on top of the NWs were circular pads. The scale bars are 1 μm.

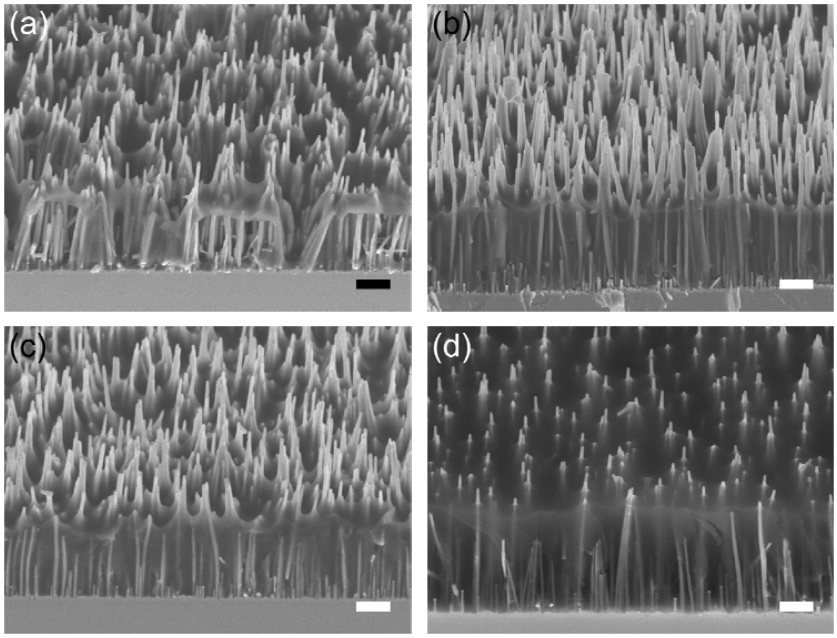

Figure 2. 45° tilted SEM images of NWs spin coated with (a) S1808, (b) SC200, (c) SU8 and (d) Cyclotene. The scale bars are 1 μm.

each sample was studied using SEM to assess the viability of each polymer as a suitable planarizing material. For reasons that will be discussed later, only the SU8- and Cyclotene-spun NW samples were chosen for further study.

Thereafter, the SU8 and Cyclotene samples were sonicated in DI water for 30 min at 40 kHz as a novel method to remove the tops of the NWs that are exposed above the polymer film, thus achieving complete planarization of the NW array, as shown schematically in figure 1(c). As shown schematically in figure 1(d), the samples then underwent reactive ion etching (RIE) to etch back the planarizing layer, thereby exposing a controlled length of the NWs to allow for subsequent contacting. The SU8-covered sample was plasma etched for 2 min with an O_2 flow rate of 28 sccm, a radiofrequency (RF) power of 100 W and a chamber pressure of 350 mTorr, while the Cyclotene-covered sample was plasma etched for 2 min with an O_2 and CF_4 flow rate of 2 sccm each, an RF power of 50 W and a chamber pressure of 150 mTorr, as recommended by previous reports [20].

Next, opaque, metal top contacts composed of 50 nm Ni, 100 nm Ge and 650 nm Au were deposited by electron beam evaporation. To prevent possible short circuits at the sample edges, the top contacts were deposited through a shadow mask consisting of an array of 800 μm-diameter circular apertures to produce discrete contact pads. A contact on the bottom of the substrate composed of 25 nm Ni, 50 nm Ge and 120 nm Au were also deposited by electron beam evaporation, as shown schematically in figure 1(e). Finally, the sample was annealed in N_2 for 30 s at 400 °C to alloy the contacts to the GaAs.

SEM analysis was used to study the morphology of the filling materials and contact after each processing step. The performance of the devices was analyzed using I–V characteristics acquired between the top and bottom contacts by a two-point probe system and a Keithley 2400 sourcemeter. I–V characteristics were used to assess whether the filling medium had successfully prevented shunts between the top and bottom contact. Finally, the two probes were placed laterally across a single contact pad and an I–V curve was measured to ensure a low sheet resistance due to effective planarization.

3. Results and discussion

Figure 1(a) shows an SEM image of the NW array directly after growth. NWs from the same growth sample were used to assess all of the polymers. Analysis of SEM images of the NW array showed that the heights of the NWs varied from ~0.5 to 5 μm while the diameters of the NWs varied between 40 and 140 nm. The density of the NW ensemble was approximately 2×10^9 cm^{-2}. Figure 2 shows SEM images of four samples each subsequently spin coated with their respective polymer (S1808, SC200, SU8 and Cyclotene). The heights of the S1808, SC200, SU8 and Cyclotene films were found to be approximately 3.3 μm, 2.7 μm, 3.3 μm and 3.5 μm, respectively. Analysis of SEM images such as those in figure 2 can be used to study the porosity and surface topography of each filling material.

Qualitative examination of porosity was performed by visual observation of the number and relative size of voids present in the filling material. While no observable voids were present for the SC200 (figure 2(b)) and SU8 (figure 2(c)) samples, there were many large voids in the S1808 layer (figure 2(a)), but only a few small voids in the Cyclotene layer (figures 1(b) and 2(d)). The presence of voids may be due to the fact that S1808 has the lowest viscosity of all the polymers examined according to the manufacturers' specifications. Although a low viscosity is generally desired for filling purposes, too much polymer may be spun off if the viscosity is too low, thus leaving voids. The presence of voids

Table 2. Mechanical properties of each filling material.

	S1808	SC200	SU8	Cyclotene
Thermal stability	—	Delaminates under anneal	Cracks under anneal Stable if under contact	Stable
Porosity	Many, large voids present	No observable voids present	No observable voids present	Few, small voids present
Roughness parameter, R_a (nm)	651	207	237	93

can be detrimental to future processing because it prevents controllable wet etching where the polymer is used as an etch stop, and has previously led to NW delamination [14]. It must also be noted from figure 2(a) that the NWs tend to bundle exclusively in the S1808 samples, indicating the presence of capillary forces as previously reported [19]. Since large voids are left behind in the S1808 layer, this leads to an imbalance of capillary forces towards the sides of NWs which are coated. As such, the NWs bundle at areas where there is polymer.

Surface topography was analyzed quantitatively by using SEM images to find the profile roughness parameter, R_a, of each sample given by [21]:

$$R_a = \frac{1}{n}\sum_{i=1}^{n}|y_i| \quad (1)$$

where y_i is the height difference between the mean line of the profile of the filling material and the ith data point (horizontal position along the polymer surface). R_a was calculated by dividing side-view SEM images taken at 10 000× magnification horizontally into $n = 48$ points each separated by 250 nm and finding y_i at each data point. The R_a values were calculated to be 651 nm, 207 nm, 237 nm and 93 nm for the S1808, SC200, SU8 and Cyclotene samples, respectively. By inspection, this trend is clearly consistent with figure 2. The large undulation of the S1808 layer in figure 2(a) is consistent with a large R_a, while it is clear from inspection of figures 2(b)–(d) that SC200, SU8 and Cyclotene have much smoother profiles with Cyclotene being the smoothest in agreement with the small calculated R_a value of 93 nm. Practically, the R_a values are of great significance because they represent the minimum top contact thickness required for good interconnection of contact material between NWs. These roughness parameter values and the porosity results from the previous discussion have been summarized in table 2. Since the S1808 layer had many large voids and a relatively large R_a due to its conformal nature, S1808 was disqualified as a potential planarizing material and no subsequent processing was done on this sample.

Before further processing of the remaining three candidates (SC200, SU8 and Cyclotene), a small piece of each sample was cleaved off and annealed at 400 °C for 30 s in N_2 to qualitatively examine the thermal stability of each polymer to subsequent high temperature processes as typically required in ohmic contact formation. The filling material is referred to as thermally stable if it maintains its structural integrity with no evidence of cracking or delamination when annealed at the aforementioned conditions. Although the Cyclotene film was found to maintain its structural integrity and morphology, this was not the case for the SC200 and SU8 films. Figure 3(a) shows severe cracking and delamination throughout the SC200 film after annealing. For this reason, SC200 was disqualified as a potential filling material. As shown in figure 3(b), the SU8 film exhibited cracks spanning tens of microns but no delamination after annealing. As shown in figure 3(c), however, such severe cracking was not observed under the contact pad planarized by SU8. It appears, therefore, that the top contact may help to prevent cracking in the case of SU8. These thermal stability results have also been summarized in table 2.

After successful planarization of the NWs with SU8 and Cyclotene, the NWs were sonicated in water. From figure 1(c), it is clear that sonication successfully removed the tops of the NWs exposed above the polymer film, thus accomplishing two goals. Firstly, this completed the perfect planarization of the NW sample. Furthermore, sonication eliminated the Au seed particle at the top of the NWs that may be detrimental in some device applications (e.g. the Au particle can reflect light away from the NWs in a photovoltaic device). Secondly, it solved the previously reported problem of an open circuit occurring if photoresist covers the tops of the NWs [10]. Sonication ensures that the top of each NW is a freshly cleaved surface with no residual polymer on it. Previously, these goals have been achieved by chemical–mechanical polishing (CMP) [12, 14]. However, sonication presents a more attractive alternative due to its simplicity, lower cost, better scalability and non-destructiveness in terms of potential delamination and cracking.

Next, RIE was examined as a method to selectively etch the polymer to a desired NW height. After sonication, the samples underwent RIE as shown in figure 1(d). RIE parameters were described in section 2. From a comparison of the SEM images in figures 1(c) and (d), it is clear that the RIE successfully uncovered the top of the NWs for contacting as intended. SEM analysis found that the density of NWs protruding out of both the SU8 and Cyclotene layers was about 5×10^8 cm^{-2} thus amounting to about 25% of all NWs. This was found to be consistent with the height distribution of the NWs.

Finally, top and bottom contacts were deposited and subsequently annealed. Figure 1(e) shows that a planar top contact was successfully deposited, while the underlying Cyclotene maintained its structural integrity after annealing, as mentioned earlier. Figure 3(c) shows an SEM image of NWs embedded in SU8 underneath a contact pad after annealing whereby only small cracks are present (indicated by the arrow in figure 3(c)), unlike the regions between contact pads as shown in figure 3(b). Therefore, as previously hypothesized,

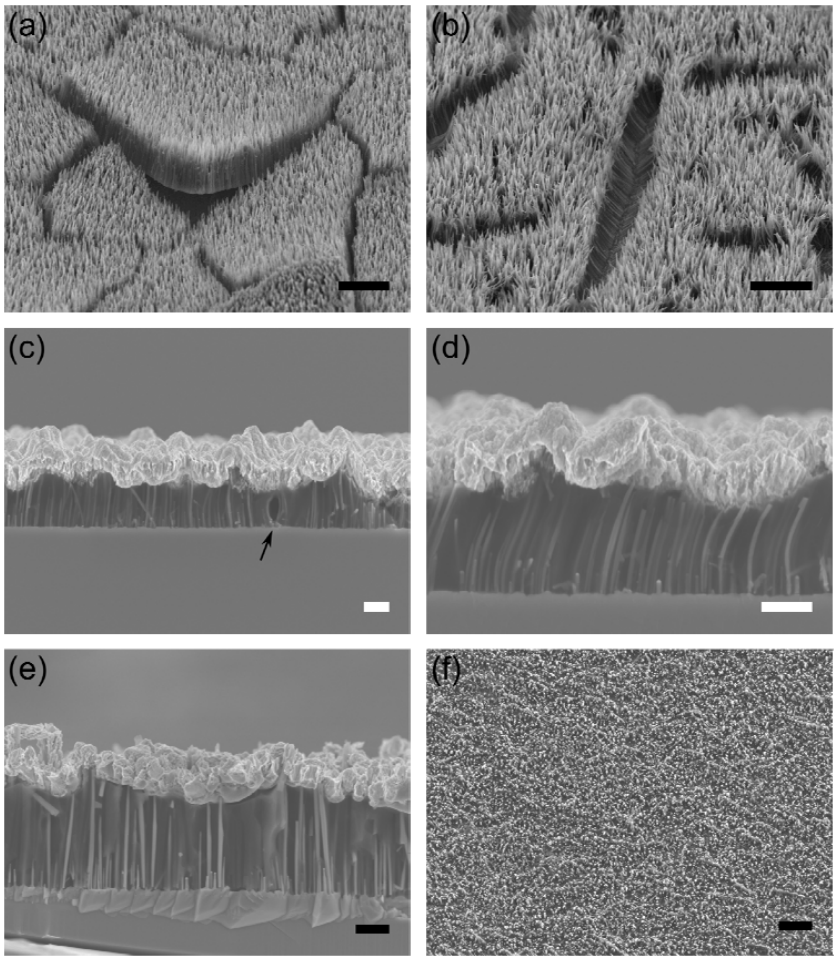

Figure 3. Post-anneal SEM images of (a) SC200 film showing severe cracking and delamination (45° tilt, 5 μm scale bar); (b) SU8 film showing major cracking at uncontacted areas (45° tilt, 5 μm scale bar); (c) SU8 film showing only minor cracking under a contact pad as indicated by the arrow (90° tilt, 1 μm scale bar); (d) SU8 film showing bowing of the NWs under a contact pad (90° tilt, 1 μm scale bar); (e) Cyclotene exhibiting no bowing of the NWs under a contact pad (90° tilt, 1 μm scale bar) and (f) Cyclotene film exhibiting no cracking even at uncontacted areas (30° tilt, 5 μm scale bar).

the SU8 layer was thermally stable under a contact pad. However, it must be noted from figure 3(d) that the NWs are bowed, indicating substantial stress in the SU8 layer. However, neither this bowing nor the aforementioned small cracks were observed in the Cyclotene sample as shown in figures 3(e) and (f). Consequently, only Cyclotene was chosen for subsequent I–V measurements.

Figure 4(c) shows the I–V measurements performed at different parts of the sample to assess the success of NW contacting. I–V characteristics were obtained from contact pads in three different locations (A, B, C) on the sample as depicted schematically in figure 4(a). The I–V analysis gave rise to four observations. Firstly, no differences in the I–V characteristics of the NWs (pad B) were observed whether the contact was deposited immediately after the sonication step or after the RIE etching step described earlier, indicating that the RIE process was not detrimental to NW contacting. Secondly, the control contact A (orange dotted line) formed on the Cyclotene film with no NWs underneath yielded negligible current. This showed that Cyclotene is insulating and effectively isolates the top and bottom contacts. Thirdly, the current passing through contact B (black dashed line) on top of the NWs is more than four orders of magnitude higher than the current passing through contact A. By comparison with the I–V characteristics from pad A, the I–V characteristics from pad B indicated that conduction occurred through the NWs as opposed to the filling material. Fourthly, the high current (blue solid line) drawn by contact C on the substrate clearly indicated the short circuited situation. When comparing the low resistance, linear I–V characteristics of contact C to the higher resistance I–V characteristics of contact B, it is clear that the NWs are not shunted, but exhibit less current possibly due to carrier depletion of the thin NWs. These depletion effects are also responsible for the rectifying nature of the I–V characteristics of pad B as compared to the linear characteristics of pads A and C. Further studies of these depletion effects are currently underway. In all, these three contacts show that the Cyclotene layer has successfully prevented both short circuits and open circuits, while permitting conduction through the NWs.

To further illustrate the effective planarization of the contact on top of the NWs, the sheet resistance of the

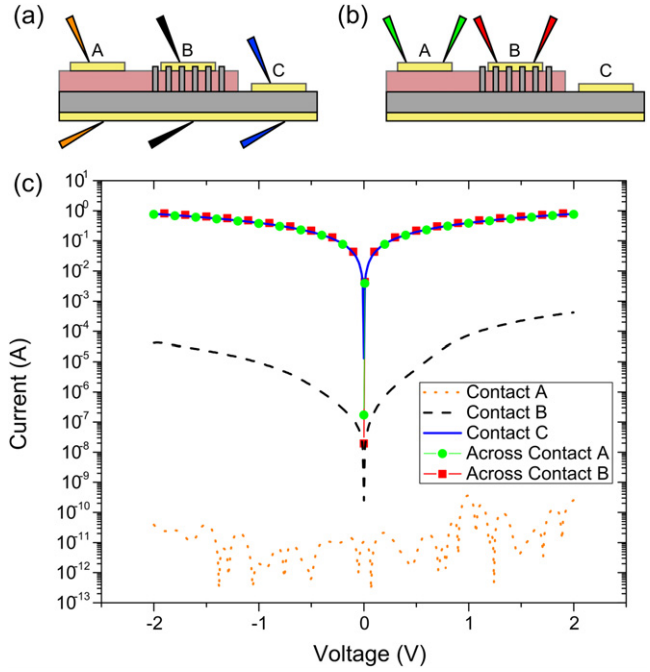

Figure 4. (a) Schematic of the three different top contacts deposited on the device with probes contacting the top and bottom of the device. (b) Schematic of the two-point probe measurement across contact pads A and B. (c) Semi-log plot of I–V characteristics between each top contact pad and the rear contact (pad A, pad B, pad C) as indicated in (a) and laterally across a single contact pad A and B as indicated in (b). The color of the probes in (a) and (b) correspond to the color of the curves in (c).

NW contacts (pad B) were estimated by simple two-point probe measurements laterally across the contact pad, as depicted schematically in figure 4(b). Figure 4(c) shows the representative I–V characteristics across contact B (red squares). The two-probe resistance laterally across the pad was found to be ∼2 Ω. I–V characteristics across contact A (green circles) yielded the same nominal two-probe resistance of ∼2 Ω. This indicates the deposition of a high quality top contact on the NWs. Additionally, further I–V measurements showed that this resistance was mainly attributed to the parasitic resistance of the measurement apparatus, indicating a negligible voltage drop across the contact pad. Therefore, planarization has been effective in creating a low sheet resistance contact on top of the NWs.

4. Conclusions

In conclusion, a consistent study of a variety of organic filling materials (S1808, SC200, SU8 and Cyclotene) was assessed for porosity, planarization and thermal stability. Qualitative analysis of the thermal stability and porosity along with quantitative analysis of the roughness of each filling material has shown that Cyclotene is best suited as an organic filling material. This analysis has in turn provided a set of standards by which future attempts at NW planarization can be judged. The novel method of removing the tops of the NWs by sonication proved to be effective in achieving complete planarization and thus stands as an attractive alternative to the conventional CMP method. Finally, a full device was successfully fabricated where the Cyclotene layer prevented both short circuits and open circuits while allowing the deposition of a low sheet resistance, planar top contact. In all, these processes and analysis can be easily repeated for future characterization and fabrication of ensemble NW devices.

Acknowledgments

The authors gratefully acknowledge financial support from the Ontario Centres of Excellence and the Natural Sciences and Engineering Research Council of Canada. The authors acknowledge useful discussions with Martin Aagesen (SunFlake A/S, Denmark).

References

[1] Wagner R S and Ellis W C 1964 *Appl. Phys. Lett.* **4** 89
[2] Bryllert T, Wernersson L-E, Löwgren T and Samuelson L 2006 *Nanotechnology* **17** S227
[3] Zheng G, Patolsky F, Cui Y, Wang W U and Lieber C M 2005 *Nat. Biotechnol.* **23** 1294
[4] Gradecak S, Qian F, Li Y, Park H-G and Lieber C 2005 *Appl. Phys. Lett.* **87** 173111
[5] Czaban J A, Thompson D A and LaPierre R R 2009 *Nano Lett.* **9** 148
[6] Kayes B M, Atwater H A and Lewis N S 2005 *J. Appl. Phys.* **97** 1
[7] Tsakalakos L 2008 *Mater. Sci. Eng.* R **62** 175
[8] Stelzner T, Pietsch M, Andra G, Falk F, Ose E and Christiansen S 2008 *Nanotechnology* **19** 295203
[9] Tsakalakos L, Balch J, Fronheiser J, Korevaar B, Sulima O and Rand J 2007 *Appl. Phys. Lett.* **91** 233117
[10] Voss L F, Shao Q, Reinhardt C E, Graff R T, Conway A M, Nikolic R J, Deo N and Cheung C L 2010 *J. Vac. Sci. Technol.* B **28** 916
[11] Novotny C, Yu E and Yu P 2008 *Nano Lett.* **8** 775
[12] Perraud S, Poncet S, Noël S, Levis M, Faucherand P, Rouvière E, Thony P, Jaussaud C and Delsol R 2009 *Sol. Energy Mater. Sol. Cells* **93** 1568
[13] Nguyen P, Ng H T, Yamada T, Smith M K, Li J, Han J and Meyyappan M 2004 *Nano Lett.* **4** 651
[14] Latu-Romain E, Gilet P, Noel P, Garcia J, Ferret P, Rosina M, Feuillet G, Levy F and Chelnokov A 2008 *Nanotechnology* **19** 345304
[15] Cirlin G, Bouravleuv A, Soshnikov I, Samsonenko Y, Dubrovskii V, Arakcheeva E, Tanklevskaya E and Werner P 2010 *Nanoscale Res. Lett.* **5** 360
[16] Tang Y, Chen Z, Song H, Lee C, Cong H, Cheng H, Zhang W, Bello I and Lee S 2008 *Nano Lett.* **8** 4191
[17] Kelzenberg M D, Boettcher S W, Petykiewicz J A, Turner-Evans D B, Putnam M C, Warren E L, Spurgeon J M, Briggs R M, Lewis N S and Atwater H A 2010 *Nat. Mater.* **9** 239
[18] Goto H, Nosaki K, Tomioka K, Hara S, Hiruma K, Motohisa J and Fukui T 2009 *Appl. Phys. Express* **2** 035004
[19] Xu C, Wang X and Wang Z L 2009 *J. Am. Chem. Soc.* **131** 5866
[20] Schier M 1995 *J. Electrochem. Soc.* **142** 3238
[21] DeGarmo E P, Black J T and Kohser R A 2007 *DeGarmo's Materials and Processes in Manufacturing* (New Jersey: Wiley)